ISSN 1990-7931, Russian Journal of Physical Chemistry B, 2016, Vol. 10, No. 4, pp. 587–594. © Pleiades Publishing, Ltd., 2016.
Original Russian Text © G.L. Agafonov, I.V. Bilera, P.A. Vlasov, Yu.A. Kolbanovskii, V.N. Smirnov, A.M. Tereza, 2016, published in Khimicheskaya Fizika, 2016, Vol. 35, No. 8, pp. 21–29.

KINETICS AND MECHANISM OF CHEMICAL REACTIONS. CATALYSIS

Formation of Soot Particles in Pyrolysis and Oxidation of Aliphatic and Aromatic Hydrocarbons: Experiments and Detailed Kinetic Modeling

G. L. Agafonov[a], I. V. Bilera[b], P. A. Vlasov[a, c, *], Yu. A. Kolbanovskii[b], V. N. Smirnov[a], and A. M. Tereza[a]

[a] *Semenov Institute of Chemical Physics, Russian Academy of Sciences, Moscow, Russia*
[b] *Topchiev Institute of Petrochemical Synthesis, Russian Academy of Sciences, Moscow, Russia*
[c] *National Research Nuclear University MEPhi (Moscow Engineering Physics Institute), Moscow, Russia*
**e-mail: iz@chph.ras.ru*

Received June 24, 2015

Abstract—Experiments on pyrolysis and oxidation of rich mixtures of various aliphatic and simple aromatic hydrocarbons in reflected shock waves have been performed. The mixtures C_2H_2/Ar, C_2H_6/Ar, C_2H_4/Ar, C_2H_4/O_2/Ar, CH_4/Ar, CH_4/O_2/Ar, C_3H_8/Ar, C_3H_6/Ar, toluene/Ar, and benzene/Ar were studied. The yield of soot and the temperature of soot particles were determined experimentally by the double-beam absorption emission method. The kinetic model of soot formation during the pyrolysis and oxidation of rich mixtures of aliphatic and aromatic hydrocarbons complemented with a set of nucleations of soot particles from both polyaromatic fragments and unsaturated aliphatic hydrocarbons was suggested. This kinetic model of soot formation was successfully tested. It describes the experimental literature data on the yield of the products of pyrolysis and oxidation of acetylene and diacetylene in a shock tube. The results of our experiments and kinetic calculations of the time, temperature, and concentration dependences are in good agreement for all hydrocarbons under study. All the kinetic parameters of the model remained strictly constant.

Keywords: pyrolysis, soot formation, spectroscopic measurements, condensation, shock waves, chemical kinetics, numerical simulation

DOI: 10.1134/S1990793116040199

INTRODUCTION

Our experimental studies and detailed kinetic calculations of formation of soot particles in the pyrolysis of aromatic hydrocarbons (benzene, toluene, and ethylbenzene [1]) and saturated aliphatic hydrocarbons (methane and propane [2–4]) showed good agreement of the experimental data and detailed kinetic calculations. However, we met certain difficulties in kinetic modeling of soot formation in the pyrolysis of mixtures of acetylene with argon, a hydrocarbon with a triple carbon–carbon bond. These difficulties were overcome by introducing an additional channel of soot particle nucleation from polyyne fragments, in particular, from diacetylene dimers in the kinetic model. The experiments performed in [5] confirmed the possibility of formation of diacetylene dimers in high concentrations in the reaction mixture.

The goal of this study was to perform the experiments and detailed kinetic calculations of soot formation during the pyrolysis and oxidation of various mixtures of aliphatic and aromatic hydrocarbons in argon in reflected shock waves and to demonstrate the predictive ability of the modified kinetic model of soot particle formation.

EXPERIMENTAL

The experiments were performed in a shock tube unit made of stainless steel with an inner diameter of 75 mm (the length of the low-pressure section was 3.2 m; the length of the high-pressure section was 1.5 m). A detailed description and the diagram of the experimental unit were given in [1]. The parameters of the gas after the passing and reflected shock wave were calculated from the initial pressure, the composition of the mixture, and the incident shock wave velocity using the theory of an ideal flow in a shock tube [6]. The incident shock wave velocity was measured on two bases using three piezoelectric pressure indicators mounted in series and made of lead zirconate–titanate.

The shock wave was generated by a spontaneous rupture of one or more aluminum diaphragms with a thickness of 0.05–0.2 mm depending on the required conditions after the incident or reflected wave. The driver gas was a mixture of helium with air in different

ratios (up to 50% content of the latter); the lower the required temperature, the greater the amount of air introduced in the driver mixture.

Soot formation was studied in the pyrolysis and oxidation of mixtures of various aliphatic and aromatic hydrocarbons strongly diluted with argon: methane, ethane, ethylene, acetylene, propane, propylene, benzene, toluene, and ethylbenzene. The procedures for the preparation of working mixtures from hydrocarbons were described in [7] and [1] for gaseous and liquid hydrocarbons, respectively. The mixtures were composed manometrically and stored in light-proof flasks.

The time profiles of the soot yield and its effective temperature after the reflected shock wave were simultaneously measured by the double-beam absorption-emission method. A detailed description of this method and all the necessary calculation formulas were given in [1, 7]. The soot yield was determined as the ratio of the concentration of the carbon atoms of the soot particle assembly to the total concentration of carbon atoms in the starting system. When determining the yield of soot, we assumed that the optical radiation absorption by soot particles is described in terms of the Mie theory using the macroscopic complex refraction index, which is independent of the particle size of soot. As the latter is much smaller than the wavelength $\lambda = 638$ nm of the light probe [8], the weakening of the beam can be described, with a good accuracy, in the Rayleigh approximation.

The temperature measurements for soot particles were performed in this study using two spatially separated channels for recording the emission and absorption of an assembly of soot particles in contrast to the traditional scheme of pyrometric measurements [1, 7]. When the characteristic rate of the thermal relaxation of particles is much higher than the characteristic heating rate due to the exothermal growth reactions and than the cooling rate due to emission, and also when the radiation intensity of chemiluminescence reactions is much smaller than the intensity of the thermal emission of particles, the effective temperature is close to the real temperature of the gas and soot particles. In the course of this study, it was verified that these conditions were well satisfied.

KINETIC MODEL

The kinetic modeling of the formation of soot particles was performed using the kinetic reaction mechanism developed in [7]. The kinetic mechanism of gas-phase reactions is based on the USC-Mech II model [4], which describes the oxidation of H_2 and CO and the high-temperature pyrolysis and oxidation of C_1–C_4 hydrocarbons. This mechanism was considerably expanded for kinetic modeling of soot formation, in particular, additional channels of formation and growth of polyaromatic hydrocarbons (up to coronene) and reactions involving C_3, C_5, and C_7 hydrocarbon fragments were included. Thus, our kinetic mechanism includes: (1) the H-abstraction/C_2H_2-addition (HACA) mechanism of the sequential growth of polyaromatic hydrocarbon molecules; (2) recombination of phenyl radicals with benzene molecules; (3) recombination of cyclopentadienyl; (4) nucleation of soot particles from unsaturated aliphatic hydrocarbons. The reasons for constructing this kinetic mechanism were given in [4, 7].

The kinetic model of soot nucleation based on recombinations of polyaromatic fragments was complemented with recombinations of the aliphatic C_8H_4 fragments to form their dimers. This modification was based on the results of studies [5, 9], in which the concentrations of these fragments were reliably measured.

It was concluded in [5] that the excited isomers of C_8H_4 are typical intermediates in the formation of higher polyynes and oligomers and that higher polyynes do not form by the direct reactions $C_4H_2 + C_2H_2 = C_6H_2 + H_2$ and $C_4H_2 + C_4H_2 = C_8H_2 + H_2$, while the linear isomers of C_8H_4 dissociate to form C_8H_2, and the branched isomers of C_8H_4 with side chains react further to form heavier oligomers or decompose into C_6H_2 molecules. The addition of C_4H_2 to the branched isomer of C_8H_4 leads to cyclization of the complex, which forms fragments containing an aromatic ring. The product is capable of further polymerization. The larger the resulting oligomer, the smaller the probability of relatively stable polyaromatic compounds with side chains.

Polyyne structures, in particular, a series of C_7H_4 and C_8H_4 isomers (polyynes and their substituted derivatives) in low-pressure rich flames of various hydrocarbons (allene, propyne, and cyclopentane) were experimentally observed in [9] by time-of-flight photoionization mass spectrometry using tunable synchrotron radiation in the UV vacuum range. In contrast to higher polyyne $C_{2n}H_2$ molecules, the possible routes of the reactions that form the C_7H_4 and C_8H_4 isomers mainly remained uninvestigated. These reactions probably occur in a similar way as the reactions that form similar but smaller fragments.

Our kinetic calculations were performed using the kinetic mechanism of soot formation developed in [4]. The latter involves the mechanism of gas-phase reactions for describing the pyrolysis and oxidation of the starting hydrocarbons, in particular, acetylene, and formation and growth of polyaromatic hydrocarbon molecules by various channels up to coronene molecules inclusive.

The basis of the mechanism of gas-phase reactions are the reactions that form polyaromatix hydrocarbons in laminar acetylene and ethylene flames (HACA mechanism). At the same time, this mechanism was complemented with additional channels of formation and growth of polyaromatic hydrocarbon molecules

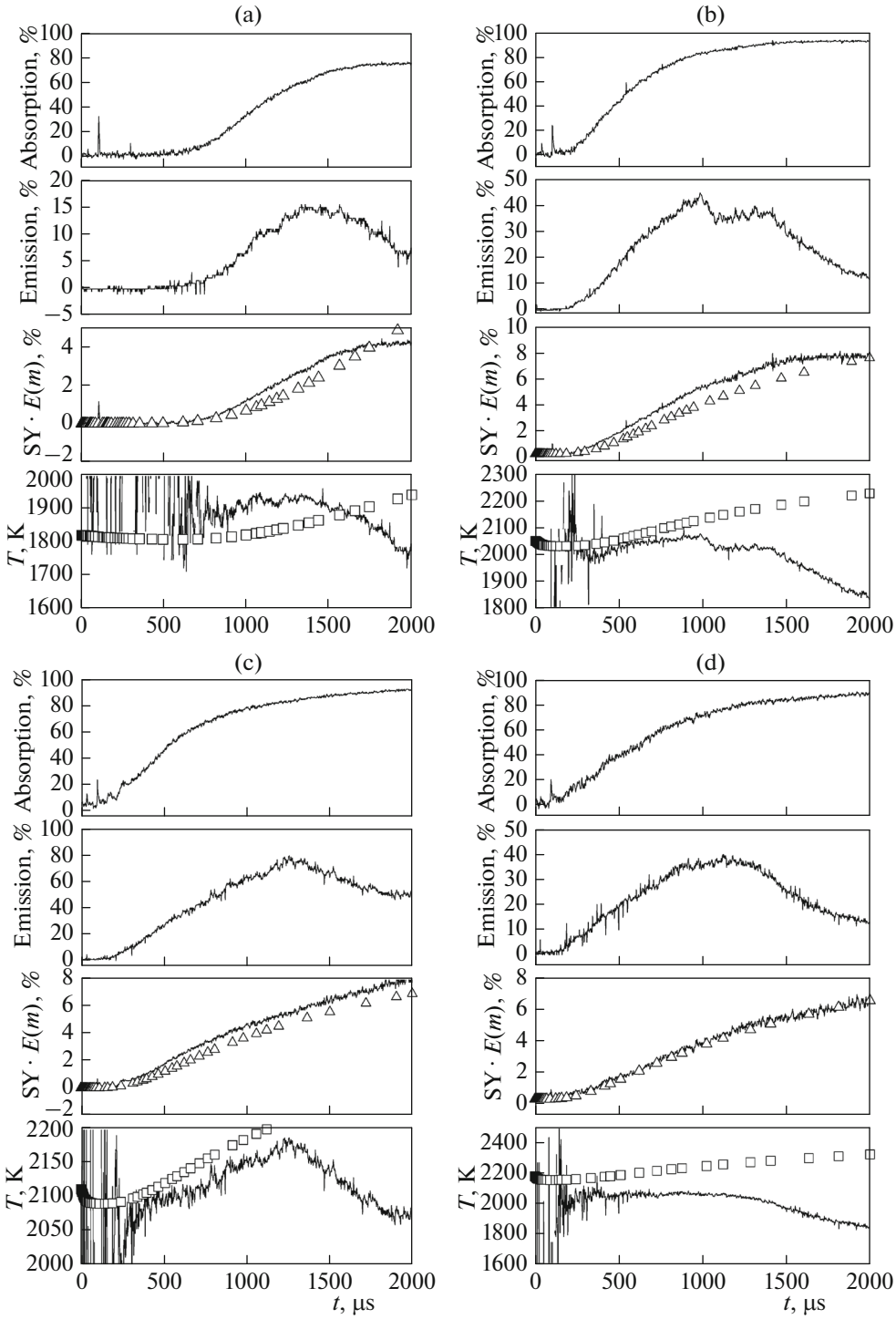

Fig. 1. Typical time profiles of the absorption and emission signals after the arrival of the reflected shock wave front to the measurement section of the shock tube and the profiles of the soot yield (SY · $E(m)$, %) and soot particle temperature obtained by processing the absorption and emission signals for a mixture of 4.8% acetylene in argon for different conditions after the reflected shock wave: (a) T_{50} = 1821 K, $[M]_{50} = 2.36 \times 10^{-5}$ mol/cm^3, P_{50} = 3.53 bar; (b) T_{50} = 2049 K, $[M]_{50} = 1.93 \times 10^{-5}$ mol/cm^3, P_{50} = 3.25 bar; (c) T_{50} = 2111 K, $[M]_{50} = 2.32 \times 10^{-5}$ mol/cm^3, P_{50} = 4.02 bar; and (d) T_{50} = 2178 K, $[M]_{50} = 2.39 \times 10^{-5}$ mol/cm^3, P_{50} = 4.27 bar. The measurements were performed at a wavelength λ = 632.8 nm. □ and △: calculated soot yield and temperature of soot particles; the lines on the soot yield and temperature axes present the results of the processing of the experimentally measured absorption and emission signals, respectively.

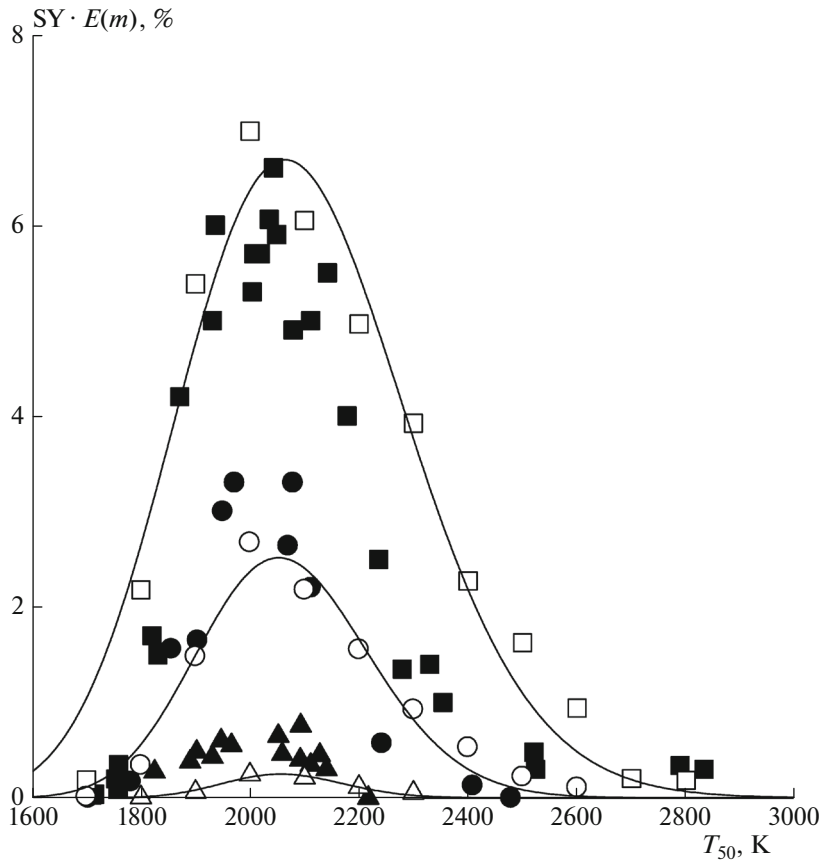

Fig. 2. Experimental and calculated temperature dependences of the soot yield in pyrolysis of three different mixtures of acetylene with argon after the reflected shock wave front: 5% (■), 3% (●), and 1.5% C_2H_2 (▲) in argon (P_{50} = 3.0–4.5 bar, $E(m)$ = 0.37, τ_{reac} = 1 ms). (■, ●, ▲) the results of experimental measurements; (□, ○, △) the results of the detailed kinetic calculations; lines: approximation of experimental data by nonlinear regression.

(up to coronene inclusive) and a set of reactions involving C_3, C_5, and C_7 hydrocarbons. Thus, the modified mechanism involves (1) the HACA mechanism (elimination of the hydrogen atom and addition of the C_2H_2 molecule)—a sequence of formation and growth reactions of polyaromatic hydrocarbon molecules due to the addition of acetylene molecules to the active sites; (2) recombinations of phenyl radicals with benzene C_6H_6 molecules; (3) recombinations of cyclopentadienyls; and (4) reactions of ring closure of aromatic rings from aliphatic hydrocarbons.

The principles of constructing the kinetic mechanism were described in [4]. The modified kinetic scheme of gas-phase reactions includes 3531 direct and reverse reactions between 300 various components; the rate constants of a series of important reactions depend on the pressure. The formation, growth, oxidation, and coagulation of soot particle nuclei and soot particles themselves were calculated by the Galerkin discrete method [10].

According to our kinetic model, the nuclei of soot particles form in radical-molecular reactions of various polyaromatic fragments starting from phenylacetylene, acenaphthalene, and ethylnaphthalene and ending with coronene radicals, and in recombinations of the unsaturated polyyne aliphatic fragments of C_8H_4. The nucleations of soot particles are assumed to be irreversible. These reactions form polyaromatic fragments containing 16–48 carbon atoms and reaction aliphatic oligomers containing initially 16 carbon atoms. All these fragments grow further and are stabilized by the formation of new chemical bonds in these complexes. The nuclei of soot particles are activated in reactions with the H and OH radicals and deactivated in reactions with H, H_2, and H_2O. The soot nuclei grow due to the addition reactions of C_2H_2, C_4H_2, and C_6H_2, whose concentration is high enough in the pyrolysis and oxidation of aliphatic and aromatic hydrocarbons and polyaromatic fragments, and due to coagulation reactions. They are oxidized in reactions with the O and OH radicals. The nuclei are transformed into soot particles in inner conversion processes, in which the number of active sites does not change. The soot particles grow in the addition reactions of C_2H_2, C_4H_2, C_6H_2, and polyaromatic fragments and are oxidized in reactions with the O and

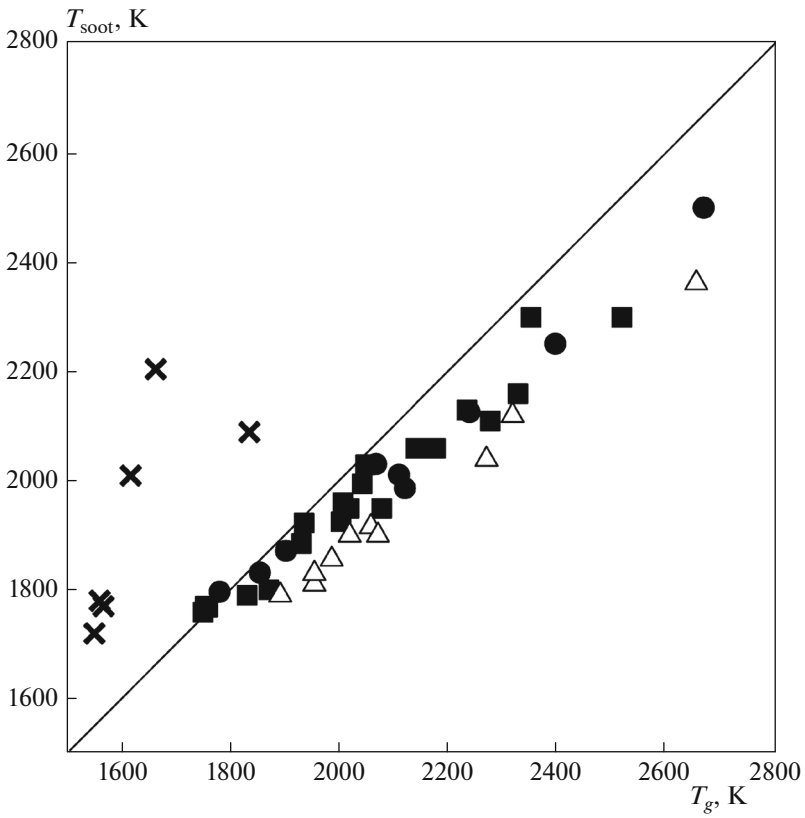

Fig. 3. Dependence of the temperature of soot particles T_{soot} formed in the pyrolysis of various mixtures of acetylene with argon for the reaction time τ_{reac} = 1 ms after the heating after the reflected shock wave on the calculated initial temperature after the reflected shock wave. Mixture compositions: 5% C_2H_2 + 95% Ar (■), 3% C_2H_2 + 97% Ar (●), 4% C_2H_2 + 1% C_3H_6O + 95% Ar (△), 5% C_2H_2 + 1.5% O_2 + 93.5% Ar (×) (C_3H_6O is acetone).

OH radicals. All soot particles are involved in coagulation reactions.

RESULTS AND DISCUSSION

The yield of soot and the temperature of soot particles were experimentally determined by the double-beam absorption-emission method, which allows simultaneous measurements of optical absorption and emission of an assembly of soot particles in the same section area of the shock tube. Figure 1 shows the typical time dependences of the absorption and emission signals after the arrival of the reflected shock wave to the measurement section and the time dependences of the soot yield and soot particle temperature obtained from these signals for soot formation in the pyrolysis of a mixture of 5% acetylene with argon under different conditions after the reflected shock wave.

The experimental dependences of the soot yield on the initial temperature after the reflected shock wave front are shown in Fig. 2 for three different mixtures of acetylene with argon. The curves are bell-shaped, which is typical for soot formation. Figure 2 clearly shows the dependence of the soot yield on the initial concentration of acetylene in the reaction mixture. Figure 3 presents the deviation of the temperature of soot particles that formed in the pyrolysis of the acetylene–argon mixtures for the reaction time 1 μs from the calculated initial temperature after the reflected shock wave front.

Since acetylene undoubtfully plays the key role in soot formation as the main component, while pyrolysis and oxidation of rich mixtures lead to the formation of acetylene in high concentrations for almost all hydrocarbons, we compared the results of calculations and experiments for acetylene and diacetylene.

The developed kinetic model of soot formation was tested by directly comparing the experimental data of [11, 12] with the results of our kinetic calculations of the yields of the products of pyrolysis and oxidation of acetylene and diacetylene. The results of this comparison are presented in Figs. 4–6. Three different C_2H_2/H_2/Ar mixtures were studied (Fig. 6): 4.0% C_2H_2 + 96% Ar, 2.5% C_2H_2 + 97.5% Ar and 2.5% C_2H_2 + 7.5% H_2 + 90.0% Ar. The results for diacetylene are shown in Figs. 4 and 5. Figure 4 presents the data on the pyrolysis of different mixtures of diacetylene with argon with hydrogen additions and without them. Figure 5 shows the results of the oxidation of the 0.4% C_4H_2 +

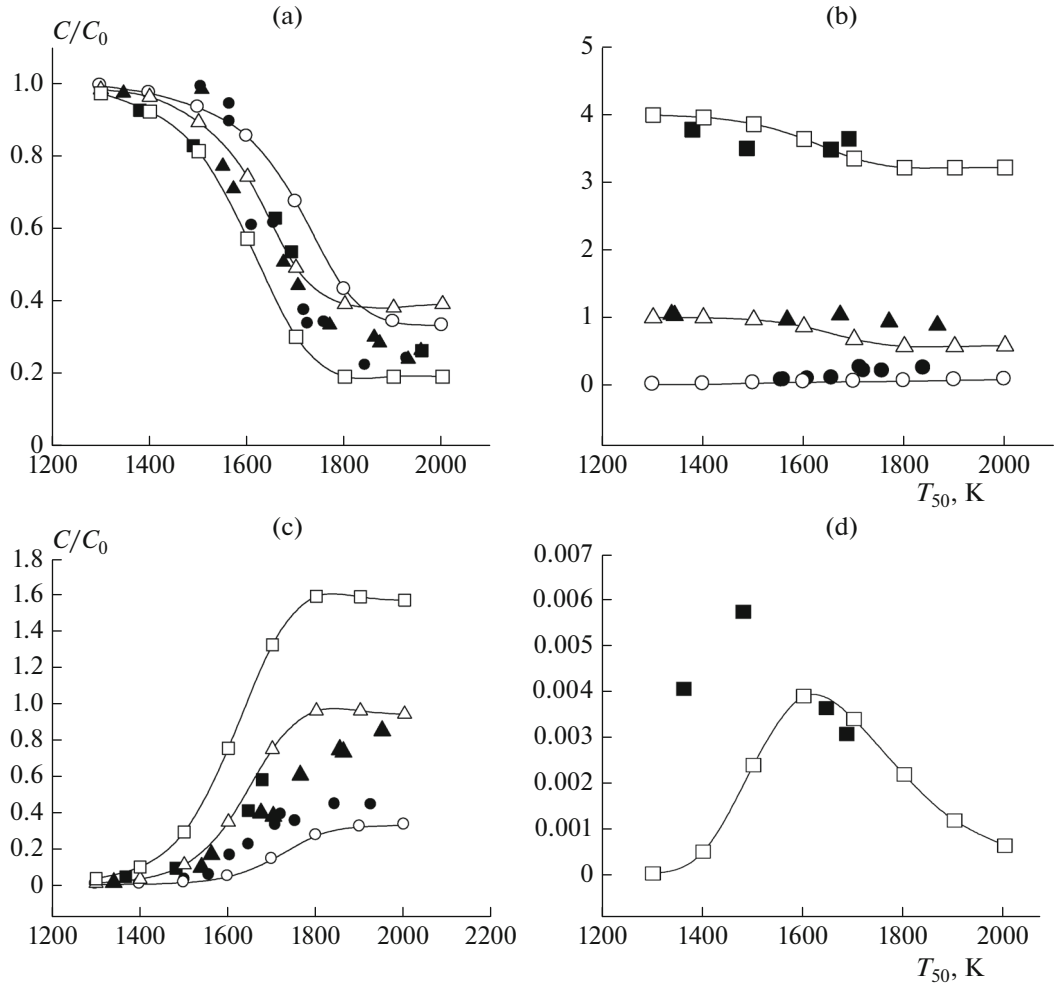

Fig. 4. Comparison of the experimental product yields (●, ▲, ■) [6] with those calculated using out kinetic model (○, △, □): (a) C_4H_2, (b) H_2, (c) C_2H_2, and (d) C_2H_4 in the pyrolysis of three different C_4H_2/H_2 mixtures in argon: 1.0% C_4H_2 + 99.0% Ar (●), 1.0% C_4H_2 + 1.0% H_2 + 98.0% Ar (▲), and 1.0% C_4H_2 + 4.0% H_2 + 95.0% Ar (■). The reaction time τ_{react} was varied depending on the temperature T_{50} after the reflected shock wave, as was done in [6]; C/C_0 is the ratio of the concentrations of the corresponding products to the initial C_4H_2 concentration in particular experiments and calculations.

0.9% O_2 + 98.7% Ar mixture. According to Figs. 4–6, the experimental and calculated data are in good agreement.

Since the temperature after the reflected shock wave front changes nonmonotonically with time (at first it quickly decreases to a certain quasistationary value, then increases, and again decreases after the arrival of the fan of rarefaction waves to the measurement section), the final soot yield is determined by this whole complex temperature profile, but not only by the temperature in the quasistationary region. Therefore, all kinetic calculations were performed for nonisothermal conditions, namely, for conditions of constant density after the reflected shock wave. A comparison of the calculated and experimental time dependences of temperature shows their good agreement. Therefore, we did not rearrange our calculated and experimental data relative to a certain effective temperature after the reflected shock wave front and used the initial calculated temperature T_{50} after the reflected shock wave for presenting our experimental and calculated temperature dependences of the parameters of soot formation.

The inclusion of the channel of soot nucleation from unsaturated aliphatic hydrocarbons in the kinetic model of soot formation in additions to the channels of soot formation from polyaromatic hydrocarbons allows us to considerably improve the kinetic description of the experimental time (Fig. 1), temperature, and concentration (Fig. 2) dependences of the soot yield not only in the pyrolysis of acetylene, but also in the pyrolysis and oxidation of all aliphatic and simple aromatic hydrocarbons under study. The suggested soot formation model adequately predicts the position of the maximum of the temperature dependence of soot yield for all hydrocarbons under study, including the pyrolysis of acetylene.

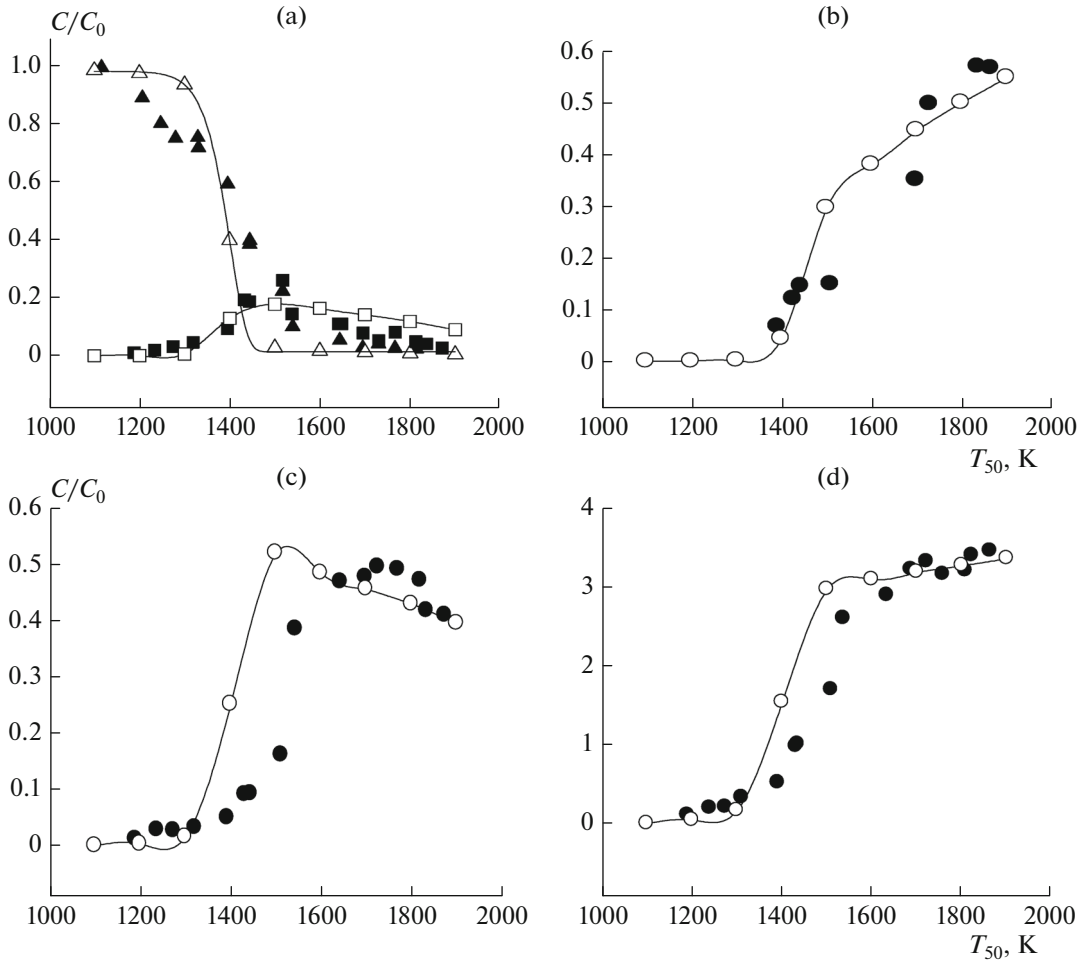

Fig. 5. Comparison of the experimental product yields from [6] (●, ▲, ■) with those calculated by our kinetic model (○, △, □): (a) C_4H_2 (▲, △), C_2H_2 (■, □); (b) H_2; (c) CO_2; and (d) CO in the oxidation of the 0.4% C_4H_2 + 0.9% O_2 + 98.7% Ar mixture. The reaction time τ_{react} was varied depending on the temperature T_{50} after the shock wave, as was done in [6]; C/C_0 is the ratio of the concentrations of the corresponding products to the initial C_4H_2 concentration in particular experiments and calculations.

Since there was a considerable scatter of the values of the optical absorption function $E(m)$ in the construction of the time and temperature dependences, the product SY · $E(m)$ of the soot yield by the optical absorption function was plotted on the ordinate. When investigating the soot formation during the pyrolysis of toluene after the reflected shock waves [1], we evaluated the optical absorption function: $E(m) = 0.37$. This value is close to the literature data: $E(m) = 0.373$ [13] and 0.259 [14].

Before the soot particles appear in the reaction system, the signal-to-noise ratio is too large to reliably determine the temperature. After the expansion fan arrived to the measurement section (after ~1100–1500 μs), the emission signal of the assembly of soot particles markedly starts to decay, which points to a decrease of the temperature of the reaction mixture in the measurement section. Details of the procedure for determining the soot yield and the temperature of soot particles are presented in [1].

CONCLUSIONS

Experiments on pyrolysis and oxidation of rich mixtures of various aliphatic and simple aromatic hydrocarbons in reflected shock waves were performed. The mixtures under study included C_2H_2/Ar, C_2H_6/Ar, C_2H_4/Ar, C_2H_4/O_2/Ar, CH_4/Ar, CH_4/O_2/Ar, C_3H_8/Ar, C_3H_6/Ar, toluene/Ar, and benzene/Ar. The soot yield and the temperature of soot particles were experimentally determined by the double-beam absorption emission method. Our experiments showed that soot formation in the pyrolysis of all aliphatic and aromatic hydrocarbons under study except pyrolysis of acetylene was accompanied by a significant decrease of temperature due to the predominance of the endothermal stages of the decay of the starting hydrocarbon. In the case of the pyrolysis of acetylene–argon mixtures, the temperature remained almost constant. The same behavior of the temperature was observed in the oxidation of rich mixtures of hydrocarbons due to the competition of the endothernal decay and exother-

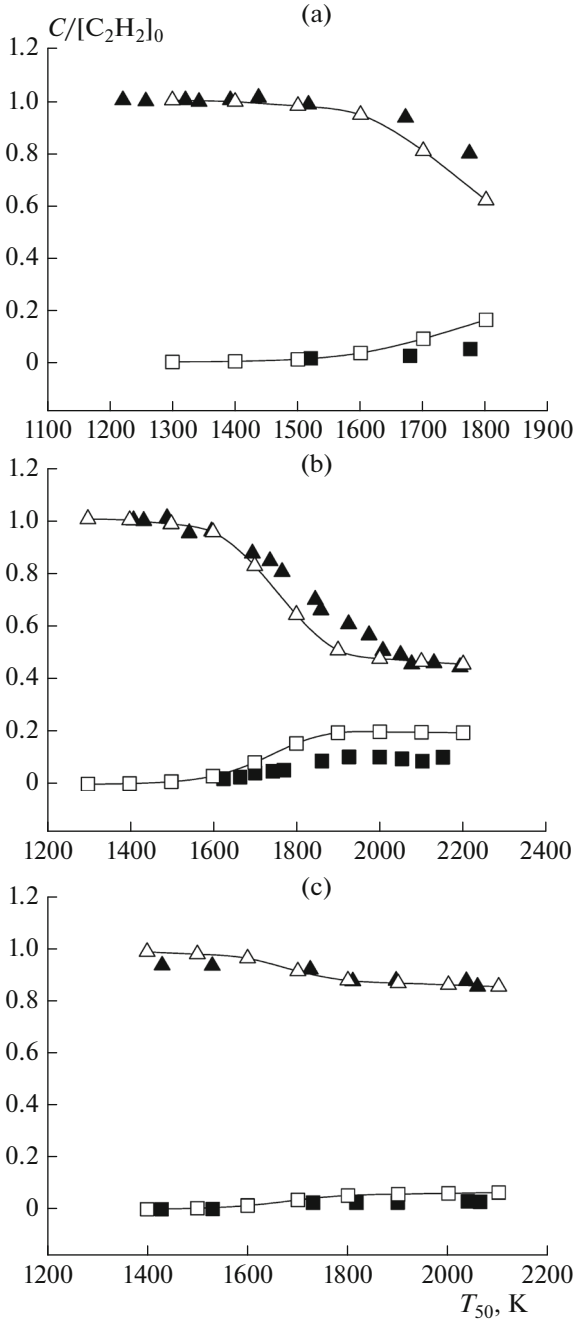

Fig. 6. Comparison of the experimental product yields from [7] (▲, ■) with those calculated in this study (△, □) for pyrolysis of different $C_2H_2/H_2/Ar$ mixtures: (a) 4.0% C_2H_2 + 96% Ar, (b) 2.5% C_2H_2 + 97.5% Ar, and (c) 2.5% C_2H_2 + 7.5% H_2 + 90.0% Ar. The reaction time τ_{react} was varied depending on the temperature T_{50} after the reflected shock wave, as was done in [7]; C/C_0 is the ratio of the concentrations of the corresponding products (▲, △ – C_2H_2; ■, □ – C_4H_2) to the initial C_2H_2 concentration in particular experiments and calculations.

mal oxidation reactions. In the oxidation of rich mixtures of acetylene with argon, the temperature grew appreciably almost immediately after the start of reaction.

Our previous kinetic model of soot formation in the pyrolysis and oxidation of rich mixtures of aliphatic and aromatic hydrocarbons was complemented with a set of soot nucleation reactions from both polyaromatic fragments and unsaturated aliphatic hydrocarbons. The suggested kinetic model of soot formation was successfully tested. It describes the published experimental data on the yield of the products of pyrolysis and oxidation of acetylene and diacetylene in a shock tube. The model also quantitatively describes our own experimental data on the time dependences of soot yield, the temperature of soot particles, and the temperature and concentration dependences of soot yield at a fixed reaction time in the pyrolysis and oxidation of the C_2H_2/Ar, C_2H_6/Ar, C_2H_4/Ar, $C_2H_4/O_2/Ar$, CH_4/Ar, $CH_4/O_2/Ar$, C_3H_8/Ar, C_3H_6/Ar, toluene/Ar, and benzene/Ar mixtures after reflected shock waves in wide temperature and pressure ranges (T_{50} = 1400–2850 K, P_{50} = 2.5–5.5 bar).

ACKNOWLEDGMENTS

This study was financially supported by the Combustion and Explosion Program (no. 31) of the Presidium of the Russian Academy of Sciences.

REFERENCES

1. G. L. Agafonov, V. N. Smirnov, and P. A. Vlasov, Kinet. Catal. **52**, 358 (2011).
2. G. L. Agafonov, A. A. Borisov, V. N. Smirnov, et al., Combust. Sci. Technol. **180**, 1876 (2008).
3. G. L. Agafonov, V. N. Smirnov, and P. A. Vlasov, Combust. Sci. Technol. **182**, 1645 (2010).
4. G. L. Agafonov, V. N. Smirnov, and P. A. Vlasov, in *Proceedings of the 33rd International Symposium on Combustion* (Combust. Inst., Pittsburgh, PA, 2011), p. 625.
5. K. H. Homann and U. Pidoll, Ber. Bunsen-Ges. Phys. Chem. **90**, 847 (1986).
6. E. V. Stupochenko, S. A. Losev, and A. I. Osipov, *Relaxation Processes in Shock Waves* (Nauka, Moscow, 1965) [in Russian].
7. G. L. Agafonov, I. V. Bilera, P. A. Vlasov, Yu. A. Kolbanovskii, V. N. Smirnov, and A. M. Tereza, Kinet. Catal. **56**, 12 (2015).
8. B. S. Haynes and H. G. Wagner, Prog. Energy Combust. Sci. **7**, 229 (1981).
9. N. Hansen, S. J. Klippenstein, P. R. Westmoreland, et al., Phys. Chem. Chem. Phys. **10**, 366 (2008).
10. P. Deuflhard and M. Wulkow, Impact Comput. Sci. Eng. **1**, 269 (1989).
11. Y. Hidaka, Y. Henmi, T. Ohonishi, et al., Combust. Flame **130**, 62 (2002).
12. Y. Hidaka, K. Hattori, T. Okuno, et al., Combust. Flame **107**, 401 (1996).
13. T. C. Williams, C. R. Shaddix, K. A. Jensen, et al., Int. J. Heat Mass Transfer **50**, 1616 (2007).
14. K. C. Smyth and C. R. Shaddix, Combust. Flame **107**, 314 (1996).

Translated by L. Smolina